

## Step over Estimation for Tool Path Generation Depending on Inclination Angle

Dr. Ahmed A. A. Duroobi

Production & Metallurgy Engineering Department, University of Technology /Baghdad

Email: ahmed\_abdulsamii7@yahoo.co.uk

Received on: 26/1/2012 & Accepted on:10/1/2013

### ABSTRACT

This research presents the theoretical model, simulation and experimental verification of the maximum stepover estimation for different cases on the machine surface profile using the end-filletted cutter in multi-axis machining. Where in this research, the equations that detect the maximum stepover at allowable scallop height value have been taking into consideration and derived to predict the tool path generation for different inclination angles of tool axis. A set of inclination angles of cutter tool axis that can machine the workpiece have been taken into consideration depending on the shape of the workpiece. The inclination angle of the tool axis, effective cutter radius, and the geometrical shape of the workpiece have been studied and experimentally verified for milling operation. The results show that the proposed model for estimating stepover at constant scallop height can predict the tool path generation for machining sculpture surfaces using CNC multi-axis machine.

**Keywords:** Step over, Tool path generation, Multi axis CNC milling.

### حساب قيمة الخطوة لتوليد مسار العدة بالاعتماد على زاوية الميلان

#### الخلاصة

في هذا البحث تم بناء موديل رياضي وعمل محاكاة إضافة إلى إجراء الجانب العملي لحساب أعلى مقدار لقيمة الخطوة التي تتحركها العدة لحالات مختلفة في حالة استخدام عدة قطع (ذات النهاية المستديرة) لماكنة قطع متعددة المحاور، حيث تم في هذا البحث اعتماد واشتقاق المعادلات اللازمة لحساب أعلى قيمة للخطوة التي تتحركها العدة عند قيمة الارتفاع التموجي المسموح بها، كذلك استخدمت هذه المعادلات للتنبؤ بتحديد أفضل مسار للعدة عند قيم مختلفة لزاوية ميلان العدة. كذلك تم الأخذ بنظر الاعتبار تحديد أفضل زاوية ميلان للعدة بالاعتماد على سطح القطعة المراد تشغيلها، إضافة إلى ذلك تم دراسة تأثير بعض المتغيرات على قيمة الخطوة التي تتحركها العدة مثل زاوية ميلان العدة، نصف القطر الفعال للعدة والشكل الهندسي للقطعة المشغلة نظرياً وعملياً. لقد أظهرت النتائج من خلال النموذج المقترح لحساب قيمة الخطوة التي تتحركها العدة عند قيمة ارتفاع تموجي ثابتة إمكانية التنبؤ بتحديد المسار الذي تتحركه العدة عند تشغيل الأشكال المختلفة للسطوح باستخدام مكانن التحكم الرقمي متعددة المحاور.

**List of Symbols:**

$R_{C1}$	The radii of the equivalent cutters at CC1.
$R_{C2}$	The radii of the equivalent cutters at CC2.
$R_a$	Effective radius of the curvature for the profile of the workpiece.
CC	Shortcut of cutter contact.
CL	Shortcut of cutter location.
$h$	The scallop height.
$R$	The cutter radius.
$R_1$	The radial distance of the cutter bottom.
$R_2$	The cutter corner radius.
$\lambda$	The lead angle of the cutter relative to the local coordinate system.
$\theta_{c1}$	The angle between $\overline{O_{c1}CC_1}$ and $\overline{O_{c1}I}$ .
$\theta_{c2}$	The angle between $\overline{O_{c2}CC_2}$ and $\overline{O_{c2}I}$ .
$\theta_{a1}$	The angle between $\overline{O_aCC_1}$ and $\overline{O_aI}$ .
$\theta_{a2}$	The angle between $\overline{O_aCC_2}$ and $\overline{O_aI}$ .

**INTRODUCTION**

The multi-axis machines add a flexibility of surface production, thus many different tool path planning and positioning methods are presented to improve the quality and to reduce the machining time at the same time. The existing CAM systems are unable to select cutters automatically for complex mould machining. Generally, the cutter is selected by a user according to his experience. As the shapes of the moulds surfaces become more and more complex, several cutters may be needed to machine a mould to improve the machining efficiency, and it is difficult for the user to select an optimal set of cutters to machine a complex mould.

Many researchers have studied the cutter selection problem [1,2 & 3], which selected cutters based on the geometry constraints. Two cutters were usually selected to machine the part. With their approaches, the smaller cutter size was first chosen as equal to the workpiece's smallest corner radius. The larger one was then chosen such that the unmachined area that remained after its use could be removed by the smaller cutter with one pass along the boundary of the finishing cutter. Since only geometric constraints were taken into account in the above researches, the number of selected cutters was restricted to one or two for each operation. The selected cutters might not be the optimal ones. To solve this problem, some researchers selected cutters based on the generated tool paths [4,5,6 & 7].

Another researchers have developed a concept of machining surface to get a continuous representation of the tool path to improve the machined surface quality [8 & 9]. They adopted in their research the case the intersection between two successive

motion of end-filletted cutter of the first cutter arc position that intersect with the arc of the second cutter position to detect the value of step over at constant scallop height value to generate tool path.

In this work, the mathematical model that estimate the maximum value of stepover at allowable scallop height value using end-filletted cutter in different types of intersection between two successive motion of the tools will be driven. The tool path generation for different inclination angles of tool axis, and a set of inclination angles of cutter tool axis that can machine the workpiece will be studied depending on the shape of the workpiece, where the workpiece surface curvature at cutting contact point will be taken into consideration in calculating the cutter location. It will produce wider tool path interval and smaller and more uniform scallops, so machining time is thus reduced dramatically.

**DEFINING THE INCLINATION ANGLE OF THE TOOL AXIS**

From Figure (1a and 1b), it can be noticed that there are two different directions of tool axis cutter. Where, Figure (1a) represents the cutting direction using multi-axis CNC milling machine which the tool axis is normal on the workpiece surface at each points of cutter contact, and the cutting will be occur by the head of cutting tool. While in Figure (1b) the tool axis is incline on the machining surface at each cutter contact points by an angle which is named lead angle ( $\lambda$ ) (lead angle is the angle that restricted between tool axis and Z-axis in the X-Z plane), and the cutting will be occur at the edge of the cutting tool.

So, from Figure (1 a, b) it can be noticed that the stepover will be changed according to the magnitude of inclination tool’s angle, and it must be derived the equations that estimate the stepover for each case ( normal and incline) so as to calculate the total length of the tool path.

**STEPOVER WHEN THE TOOL IS NORMAL ON THE MACHINING SURFACE**

The equation that estimates the magnitude of stepover when the tool axis is normal on the machining surface was derived in details in reference.[10]

Where, from Figure (2). the final equation of step over can be written as:

$$S = R_{c1} \sin(\theta_{C1}) + R_{c2} \sin(\theta_{C2}) + 2R_1 \quad \dots (1)$$

Where:

S= Stepover.

$R_{c1}, R_{c2}$  = Effective tool cutter radius.

Where  $R_{c1}$  &  $R_{c2}$  can be calculate according to equation bellow:[11]

$$R_c = \frac{R_1}{\sin(\lambda)} + R_2 \quad \dots (2)$$

Since ( $R_1$ ) are the radial distance of the cutter bottom and ( $R_2$ ) the cutter corner radius. So to calculate the value of stepover the magnitude of the angle ( $\theta_{ci}$ ) must be detected first, as follows:

$$\cos(\theta_{C1}) = \frac{R_{c1} - h}{R_{c1}} \Rightarrow \theta_{C1} = \cos^{-1}\left(\frac{R_{c1} - h}{R_{c1}}\right) \quad \dots (3)$$

$$\cos(\theta_{C2}) = \frac{R_{c2} - h}{R_{c2}} \Rightarrow \theta_{C2} = \cos^{-1}\left(\frac{R_{c2} - h}{R_{c2}}\right) \quad \dots (4)$$

### CALCULATING THE STEPOVER WHEN THE TOOL IS INCLINED ON THE MACHINING SURFACE

The equations that will be derived in this research to detect the value of the stepover must be divide into two parts, the first one is for plane surface, and the second is for sculpture surface. As follows:

- **Plane surface (Flat surface):**

When the tool is incline on the surface machining, the magnitude of stepover will be changed according to the value of lead angle ( $\lambda$ ), and before derive the equations that calculate stepover, it must be first detect the place of intersection of two consequent points for two sequential motion of the end-filletted cutter, and this mean the intersection of two sequential motion must be divided into three cases:

- a. The intersection between two successive motions occurred when the arc of the first cutter position intersect with the arc of the second cutter position. Figure(3a).
- b. The intersection between two successive motions occurred when the arc of the first cutter position intersect with the line of the second cutter position. Figure(3b).
- c. The intersection between two successive motions occurred when the line of the first cutter position intersect with the line of the second cutter position. Figure(3c).

From Figures (3 a, b & c), it can be noticed that the case of Figure (3a) usually occurred when the value of lead angle ( $\lambda$ ) is small, and the case of Figure (3c) occurred when the value of lead angle ( $\lambda$ ) is big. While the case of Figure (3b) occurred when the value of lead angle ( $\lambda$ ) is middle, taking into consideration the value of allowable scallop height and the dimension of the cutter geometry.

**a. Generating stepover through the intersection of two arcs**

For the intersection of two arcs it can be divide the derivation into two parts:

**First:** when the intersection occurred at the second arc of the first cutter position to the second arc of the second cutter position in side view as shown in Figure (4).

Actually, this case occur when the magnitude of scallop height is very small, and the end-filletted cutter will behave as a ball cutter with radius equal to ( $R_2$ ). Then the

value of stepover can be calculated like the same procedure when the tool axis normal on the machining surface from equation (1 to 4) except a difference in stepover equation that is not include the value of  $(RI)$  as follows:

$$S = R_{c1} \sin(\theta_{c1}) + R_{c2} \sin(\theta_{c2}) \quad \dots (5)$$

**Second:** when the intersection occurred at the second arc of the first cutter position to the first arc of the second cutter position in side view as shown in Figure (5).

In this case the equation of stepover can be derived as follow:

$$S = a + b + c \quad \dots (6)$$

$$a = R_{c1} \sin(\theta_{c1}) \quad \dots (7)$$

Where  $R_{c1} = R_2$ ,  $\theta_{c1}$  can be obtained from equation (3).

$$b = R_{c2} \sin(\theta_{c2}) \quad \dots (8)$$

Where  $R_{c2} = R_2$

$$\theta_{c2} = \cos^{-1}\left(\frac{d-h}{R_{c2}}\right)$$

And  $d = R_{c2} + 2R_1 \sin(\lambda) = R_2 + 2R_1 \sin(\lambda)$

$$c = 2R_1 \cos(\lambda) \quad \dots (9)$$

**b. Generating stepover through the intersection of arc and line:**

From the Figure (6a) the value ( $R_{c2}$ ) is not equal to  $(R_2)$ , and the equation of stepover can be derived as follows:

$$S = a + b + c \quad \dots (10)$$

$$a = R_{c1} \sin(\theta_{c1}) \quad \dots (11)$$

Where  $R_{c1} = R_2$ ,  $\theta_{c1}$  can be obtained from equation (3).

$$b = R_2 \sin(\lambda) \quad \dots (12)$$

$$c = j / \tan(\lambda) \quad \dots (13)$$

To find the value of ( $j$ ), it must be first find the value of ( $d$ ) and ( $e$ ) from Figure (6b), as follows:

$$d = R_2 \cos(\lambda)$$

$$e = R_2 - d$$

$$\text{Then } j = h - e$$

**c. Generating the stepover through the intersection of two lines**

From the Figure (7 a & b) the values ( $R_{c1}$ ) and ( $R_{c2}$ ) are not equal to ( $R_2$ ), and the equation of stepover can be derived as follows:

$$S = a_1 + b_1 + b_2 + a_2 \quad \dots (14)$$

$$a_1 = R_{c1} \sin(\theta_{c1}) \quad \dots (15)$$

Where  $\theta_{c1} = \lambda$  (from Figure 7a).

$$b_1 = c \cos(\lambda) \quad \dots(16)$$

To find the value of ( $c$ ) from Figure (7a) as follows:

$$d_1 = R_{c1} \cos \theta_{c1} = R_2 \cos \lambda$$

$$\text{And } e_1 = R_{c1} - d = R_2 - d$$

$$\text{Then } c = h - e_1$$

$$a_2 = R_{c2} \sin(\theta_{c2}) \quad \dots (17)$$

Where  $\theta_{c2} = \lambda$  (from Figure 7b).

$$b_2 = c \cos(\lambda) \quad \dots (18)$$

To find the value of ( $c$ ) from Figure (7b) as follows:

$$d_2 = R_{c2} \cos \theta_{c2} = R_2 \cos \lambda$$

$$\text{And } e_2 = R_{c2} - d = R_2 - d$$

$$\text{Then } c = h - e_2$$

Since the maximum allowable scallop height is specified as  $h_{max}$ , i.e.  $h = h_{max}$ . Finally, the maximum allowable path interval which is guaranteed that the scallop height is controlled under  $h_{max}$  can be obtained. It can be found that the maximum allowable path interval is derived as a function of the maximum allowable scallop height ( $h$ ), and the radius of the equivalent end-filletted cutter ( $R_{c1}$  and  $R_{c2}$ ), and then it can be detect which lead angle and then stepover can give us a minimum machining time in best surface finish for the plane surfaces.

• **Sculpture surface**

Simply, any surface include concave and convex form called sculpture surface, and the complexity of the sculpture surface depend on the number of concave and convex shapes that contained in this surface.

Where, in the present research the equations that calculate the magnitude of stepover for concave and convex mode will be derived, and it must be taken into consideration that the derived equation deal with shapes having radius ( radius of curvature for concave and convex shape), and this mean that just case (a) that was mentioned previously can be applied, cause this case dealt with the arc of the end-filletted cutter (first and second arcs). So it can be make relation between these arc ( $R_{c1}$  and  $R_{c2}$ ) and radius of the curvature ( $R_a$ ) of the surface machining as shown in Figure (8).

Otherwise, if the case (b and c) applied at concave and convex surface, that mean gouge and chordal deviation will be occur on the machining surface, which they restrict between the curve of the workpiece and the line of the cutter that was mentioned in case (b and c) previously.

So, the equation of stepover can for concave and convex form can be derived as follow:

**CONCAVE FORM**

From Figure (9), the equation of the stepover can be written as follows:

$$S = 2R_a \cdot \sin\left(\frac{\theta_{a1} + \theta_{a2}}{2}\right) \quad \dots (19)$$

$$\overline{O_a I} = \sqrt{[R_{ci} \cdot \sin(\theta_{ci})]^2 + [(R_{ai} - R_{ci}) + (R_{ci} \cdot \cos(\theta_{ci}))]^2} = R_a - h \quad \dots (20)$$

So from the equation (20), the value of ( $\theta_{c1}$ ) and ( $\theta_{c2}$ ) can be obtained as follows:

$$\therefore \cos(\theta_{c1}) = \frac{-R_{c1}^2 - (R_a - R_{c1})^2 + (R_a - h)^2}{2(R_a - R_{c1})R_{c1}} \quad \dots (21)$$

And

$$\cos(\theta_{c1}) = \frac{-R_{c2}^2 - (R_a - R_{c2})^2 + (R_a - h)^2}{2(R_a - R_{c2})R_{c2}} \quad \dots (22)$$

So from equations (21) and (22) respectively and from the Figure of concave form, the value of angle ( $\theta_a$ ) can be calculated as bellow:

$$\theta_{a1} = \cos^{-1}\left(\frac{R_a - (R_{c1} - R_{c1} \cos(\theta_{c1}))}{(R_a - h)}\right) \quad \dots (23)$$

And

$$\theta_{a2} = \cos^{-1}\left(\frac{R_a - (R_{c2} - R_{c2} \cos(\theta_{c2}))}{(R_a - h)}\right) \quad \dots (24)$$

### CONVEX FORM

From Figure(10), the equation of the stepover can be written as follows:

$$S = 2R_a \cdot \sin\left(\frac{\theta_{a1} + \theta_{a2}}{2}\right)$$

$$\therefore \overline{O_a I} = \sqrt{[R_{c1} \cdot \sin(\theta_{c1})]^2 + [R_{a1} + (R_{c1} - (R_{c1} \cdot \cos(\theta_{c1})))]^2} = R_a + h \dots (25)$$

So from the equation (25) , the value of ( $\theta_{c1}$ ) and ( $\theta_{c2}$ ) can be obtained as follows:

$$\therefore \cos(\theta_{c1}) = \frac{R_{c1}^2 + (R_a + R_{c1})^2 - (R_a + h)^2}{2(R_a + R_{c1})R_{c1}} \quad \dots (26)$$

And

$$\cos(\theta_{c1}) = \frac{R_{c2}^2 + (R_a + R_{c2})^2 - (R_a + h)^2}{2(R_a + R_{c2})R_{c2}} \quad \dots (27)$$

From equations (26) and (27) respectively and from the Figure of convex form, the value of angle ( $\theta_a$ ) can be calculated as follow:



$$\theta_{a1} = \cos^{-1} \left( \frac{R_a + (R_{c1} - R_{c1} \cos(\theta_{c1}))}{(R_a + h)} \right) \quad \dots (28)$$

And

$$\theta_{a2} = \cos^{-1} \left( \frac{R_a + (R_{c2} - R_{c2} \cos(\theta_{c2}))}{(R_a + h)} \right) \quad \dots (29)$$

Since the maximum allowable scallop height is specified as  $h_{max}$ , i.e.  $h = h_{max}$ , the values of  $(\theta_{a1})$  and  $(\theta_{a2})$  can be obtained from equations (23, 24, 28 and 29), respectively.

So, substituting  $(\theta_{a1})$  and  $(\theta_{a2})$  into equation (19), the maximum allowable path interval which is guaranteed that the scallop height is controlled under  $h_{max}$  can be obtained. It can be found that the maximum allowable path interval is derived as a function of the maximum allowable scallop height ( $h$ ), and the radius of surface curvature ( $R_a$ ), and the radius of the equivalent tours cutter ( $R_{c1}$  and  $R_{c2}$ ).

During the machining, the maximum allowable scallop height remains constant, but the radius of surface curvature ( $R_a$ ), and the radii of the equivalent tours cutter ( $R_{c1}$  and  $R_{c2}$ ) are changing along the tool paths and depending on the magnitude of lead angle ( $\lambda$ ) that was changed in the present work into five value  $\lambda = [0^\circ, 15^\circ, 30^\circ \text{ and } 45^\circ]$ . Finally, it can be detect which lead angle and stepover can give us a minimum machining time in best surface finish for the sculpture surfaces.

### **SIMULATION AND EXPERIMENTAL WORK**

In the present work Matlab program was used so as to estimate the required parameters and the flow chart will explain the steps of the program that was built up, as shown in Figure(11):

Also, UGS program have been utilized in the present research so as to simulate the process of machining before make the experimental work, where Figures (12, 13, 14 and 15) shown some pictures that explained the simulation processes occurred using UGS program for machining in multi-axis.

Where, parallel tool path have been selected to generate a clear and measurable surface profile which is suitable to get an accurate measurement for the values of scallop height and step over by using the electronic microscope. Also, The simple trimmed surfaces have been used in present work to facilitate the process of measuring step over and make the comparison between experimental results with the theoretical results of the proposed mathematical model.

Multi-axis CNC machine have been utilized to implement the experimental work in the present research using end-filletted cutter ( $R1=1mm$  ,  $R2=2mm$ ), in CAD/CAM laboratory / mechanical department in Nanjing University for Aeronautics and Astronautics in China. And Figure (16 a, b and c) shows the specimens that implemented in the experimental work.

## CONCLUSIONS

The mathematical model and experimental work can be displayed in curve form as shown in Figures (17 and 18). Where this research presents the theoretical model, simulation and experimental verification of the maximum stepover estimation at allowable scallop height value for different cases on the machine surface profile using the end-filletted cutter. Inclination angle of the tool axis, effective cutter radius, different geometrical shape of the workpiece, have been studied and experimentally verified, and the analysis result matched the experimental result very well.

It can be concluded that the present model for estimating stepover at constant scallop height will be useful to predict the tool path generation for machining different shapes using multi-axis machine. Also, changing angle of the tool axis ( $\lambda$ ) in a specific value will lead to decrease the machining time and cost of machining, and to avoid gouging or interference between the tool axis and the surface of the work piece. The developed mathematical model to generate the tool path at different lead angle can be used to estimate the maximum value of stepover at constant scallop height.

## REFERENCES

- [1]. Bala, M. T.C. Chang, "Automatic Cutter Selection and Optimal Cutter Path Generation for Prismatic Parts", *Int. J. of Prod. Research*, vol. 29, pp. 2163- 2176, 1991.
- [2]. Yang, D.C.H. Z. Han, "Interference Detection and Optimal Tool Selection in 3-axis NC Machining of Free-form Surfaces", *Computer-Aided Design*, vol. 31, pp. 303-315, 1999.
- [3]. Yamazaki, K. Y. Kawaharh, J.C. Jeng, H. Aoyama, "Autonomous Process Planning With Real-time Machining for Productive Sculptured Surface Manufacturing Based on Automatic Recognition of Geometric Features", *Annals of the CIRP*, vol. 44, pp. 439-444, 1995.
- [4]. Lee, K. T.J. Kim, S.E. Hong, "Generation of Tool path With Selection of Proper Tools for Rough Cutting Process", *Computer-Aided Design*, vol. 26, pp. 822-831, 1994.
- [5]. Kyoung, Y.M. K.K. Cho, C.S. Jun, "Optimal Tool Selection for Pocket Machining in Process Planning", *Computers in Ind. Eng.*, vol. 33, pp. 505-508, 1997.
- [6]. Ding, X. M. Y. Q. Lu, P. L. Liu, "Optimal cutter selection for complex mould machining", *SIM. Tech technical reports*, vol. 6 Number 1, 2005.
- [7]. Klaus Schützer, Eberhard Abele, Carsten Stroh, "Using Advanced CAM-Systems for Optimized HSC-Machining of Complex Free Form Surfaces", *J. of the Braz. Soc. of Mech. Sci. & Eng*, Vol. XXIX, No. 3 / 313, 2007.
- [8]. Tournier, C. E. Duc, "A Surface Based Approach for Constant Scallop Height Tool-Path Generation", *Int. J Adv. Manuf. Technol*. Vol.19, 318–324, 2002.
- [9]. Tournier, C. E. Duc, "Iso-scallop tool path generation in 5-axis milling", *Int. J Adv. Manuf. Technol*. Vol.25, 867–875, 2005.
- [10] Ahmed A.A. Duroobi, "Scallop height emulation for multi-axis CNC milling operation", PhD thesis, Iraq, Baghdad, University of Technology, 2009.

[11]. Ahmed A.Abdulwahhab, Jamal H. Mohamed, Bahha I. Kazem, "The Mathematical description of end mill cutters and effective radius of tool geometry on multi-axis milling", Eng. & Tech. Journal, Vo.28, No.8, 2010.

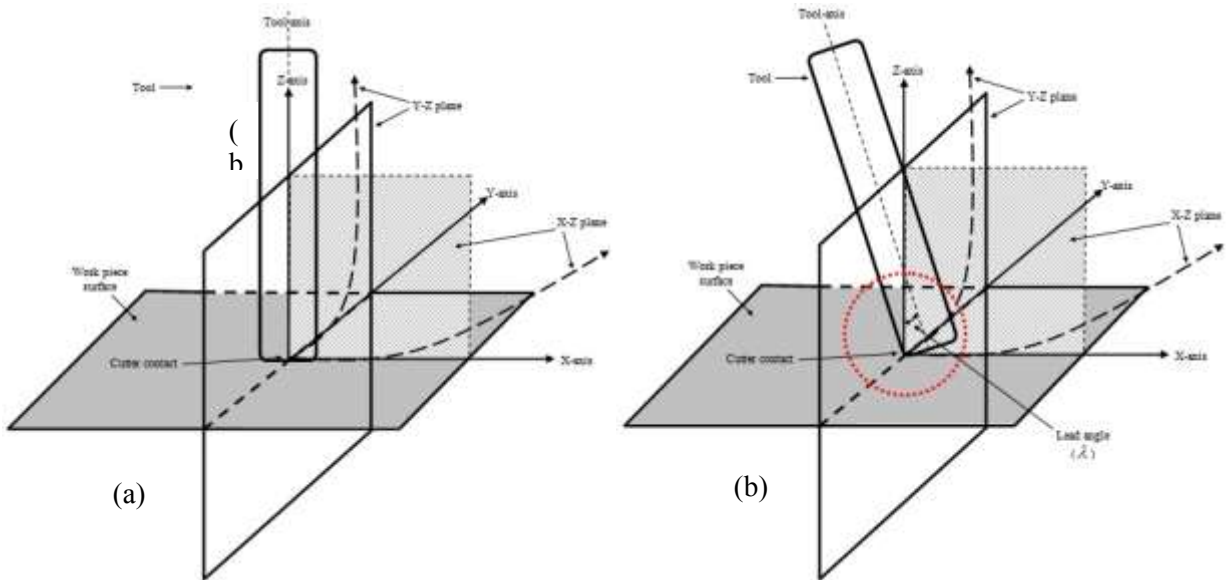
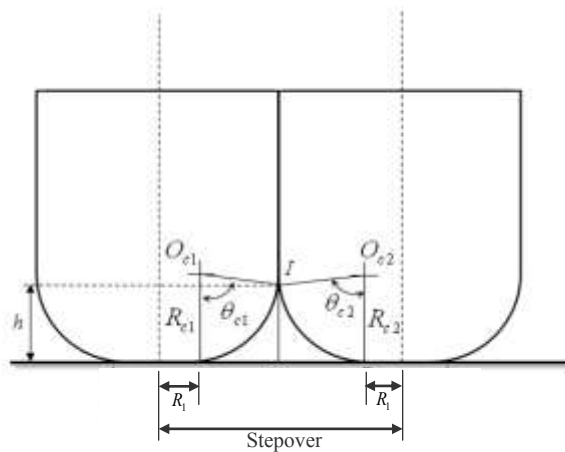


Figure (1) (a) the cutting direction normal on the workpiece. (b) tool axis is incline on the machining surface by lead angle.



Figure(2) The stepover when the tool axis is normal on the machining surface.[8]

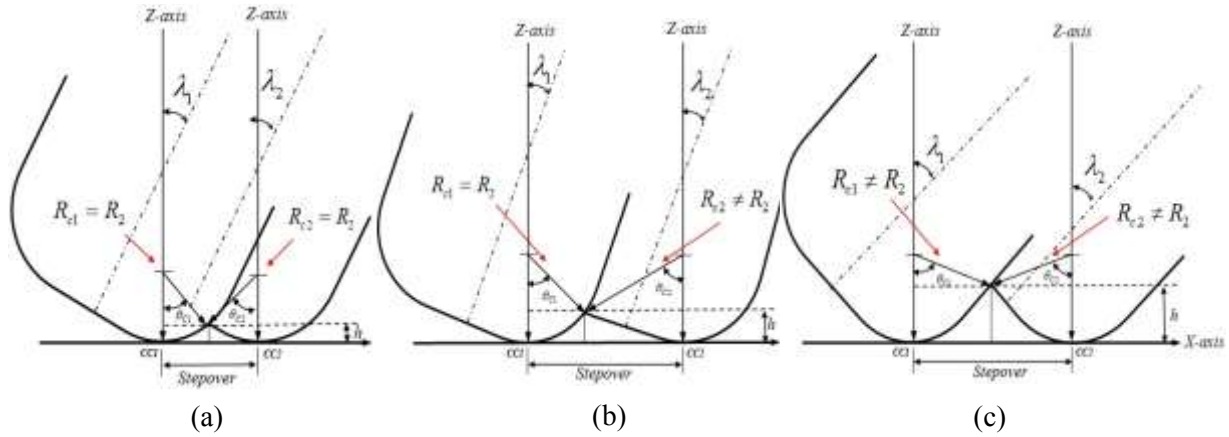


Figure (3 a, b & c). The types of intersection between two successive motion of end-filleted cutter.

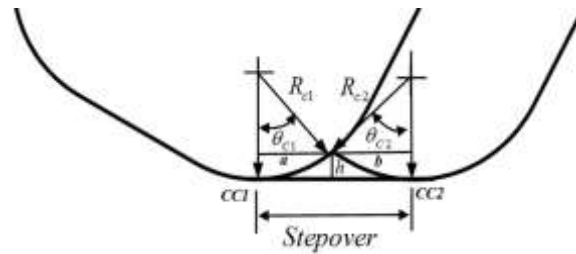


Figure (4) The intersection at the second arc of the first cutter position to the second arc of the second cutter

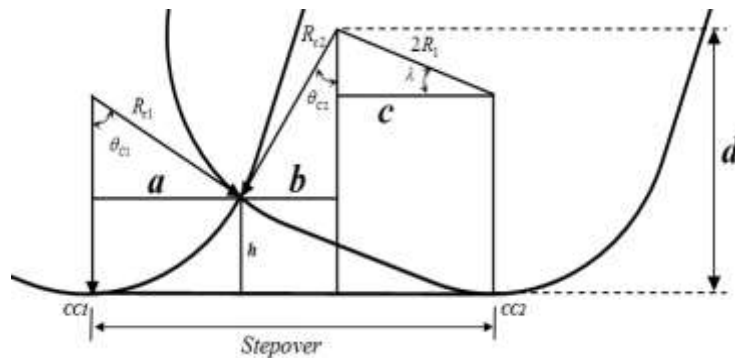


Figure (5) The intersection at the second arc of the first cutter position to the first arc of the second cutter position.

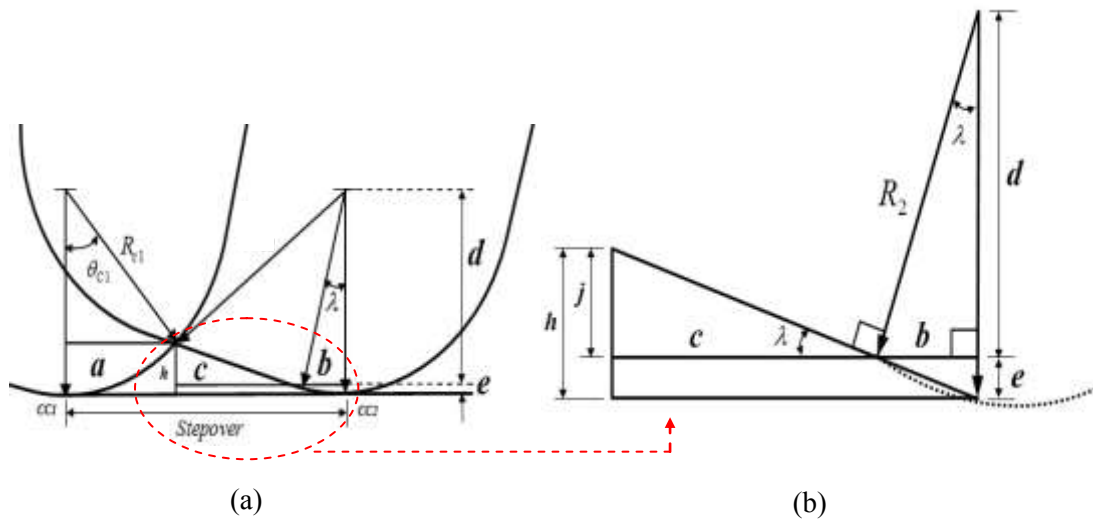


Figure (6) The intersection between two successive motion occurred when the arc of the first cutter position intersect with the line of the second cutter position.

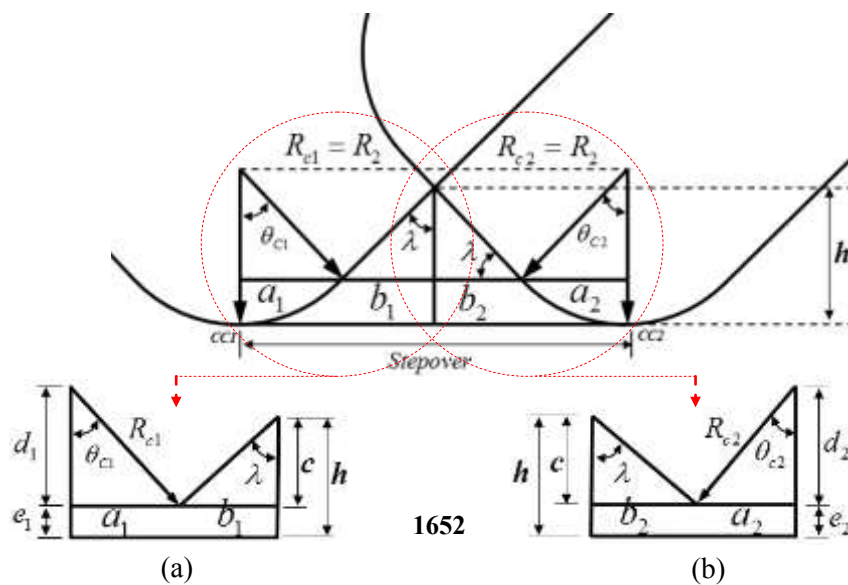


Figure (7 a & b). The intersection between two successive motion (from  $cc_1$  to  $cc_2$ ) when the line of the first cutter position intersect with the line of the second cutter position.

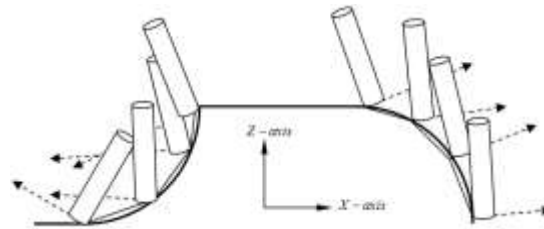


Figure (8) Concave and convex form in side view.

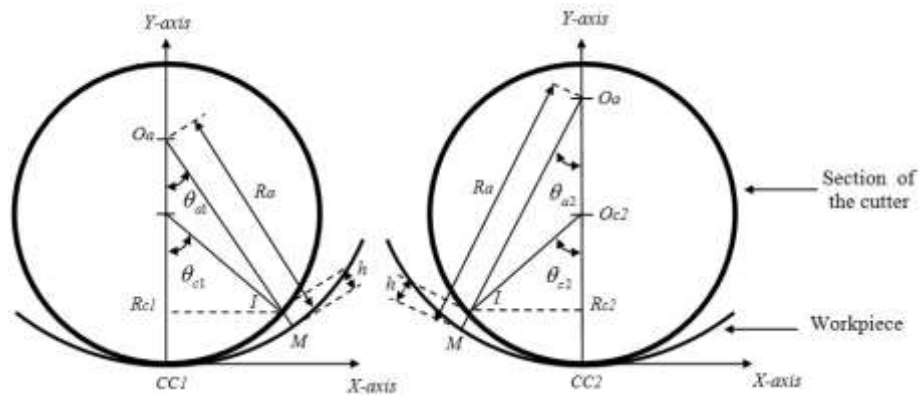
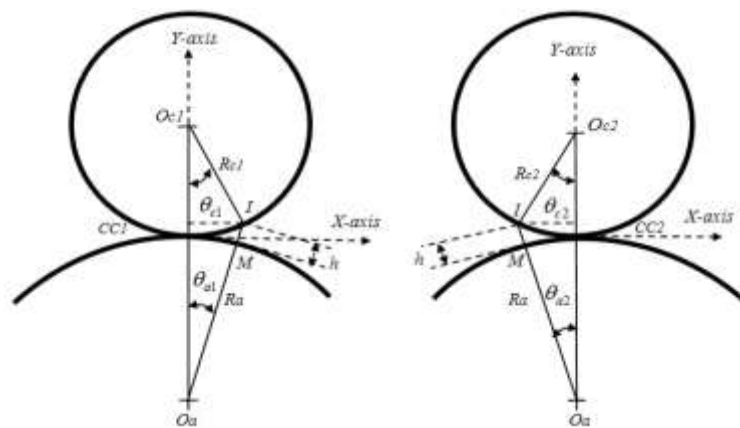
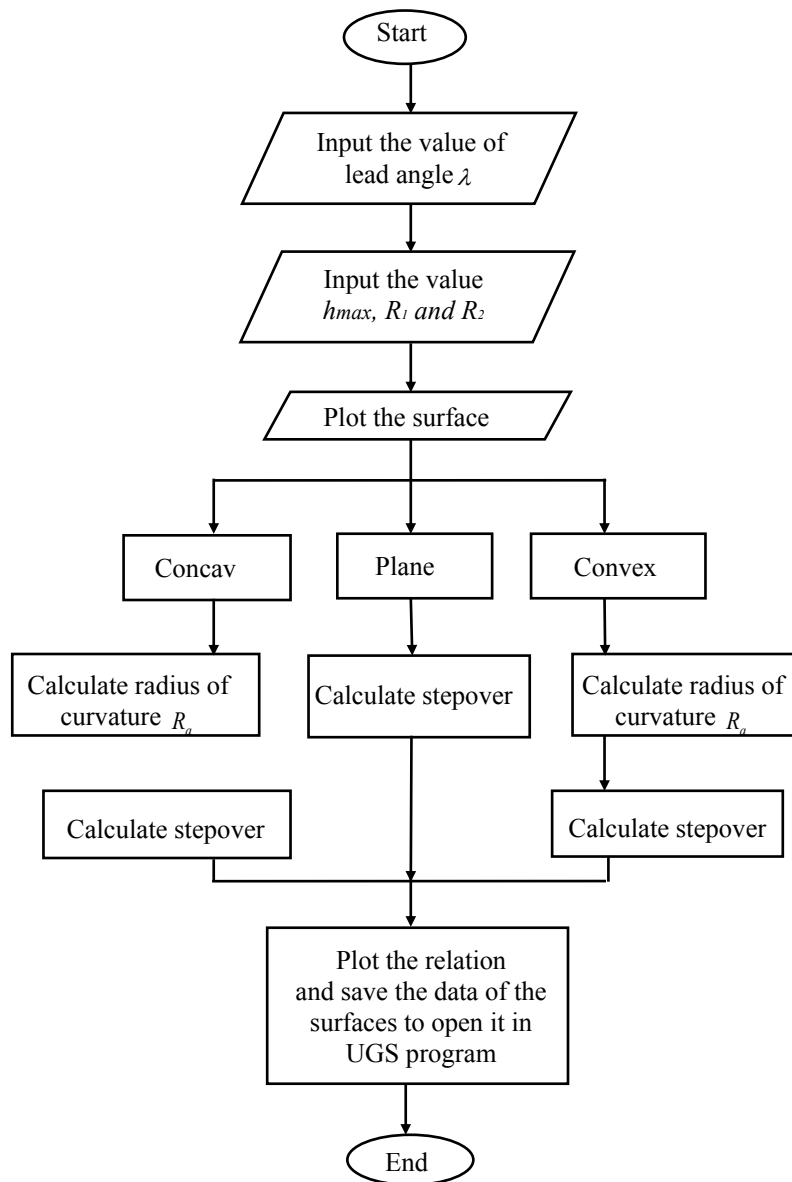


Figure (9) the connection between the cutter and the machining surface on concave form in top view.



Figure(10) The connection between the cutter and the machining surface on convex form in top view.



Figure(11) Flowchart shownn the steps of the program that was built in the present research.



Figure (12 a, b and c). The simulation processes using UGS software for the plane, concave and convex surface respectively.

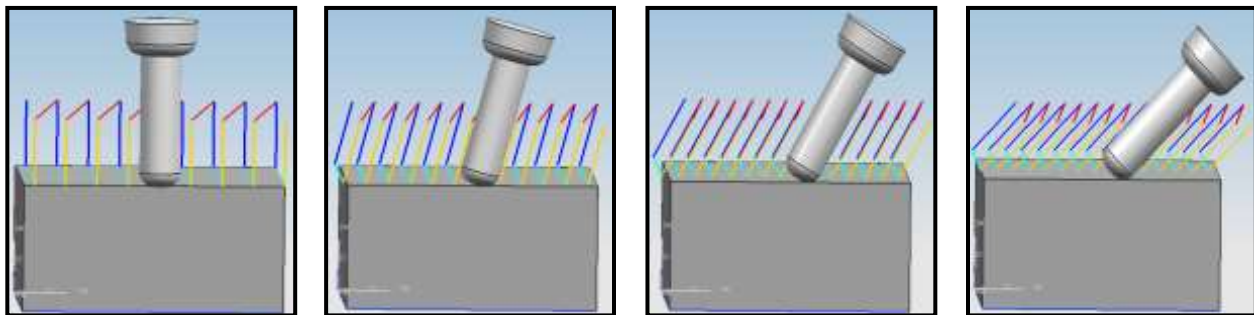


Figure (13 a, b, c and d). The tool path generation of multi-axis CNC milling operation For  $[\lambda = 0^\circ, 15^\circ, 30^\circ \text{ and } 45^\circ]$  respectively for the plane surface.

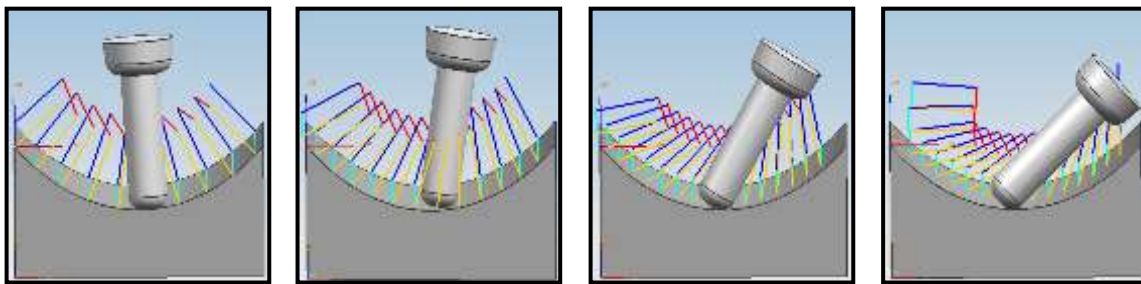


Figure (14 a, b, c and d). The tool path generation of multi-axis CNC milling operation For  $[\lambda = 0^\circ, 15^\circ, 30^\circ \text{ and } 45^\circ]$  respectively for the concave surface.

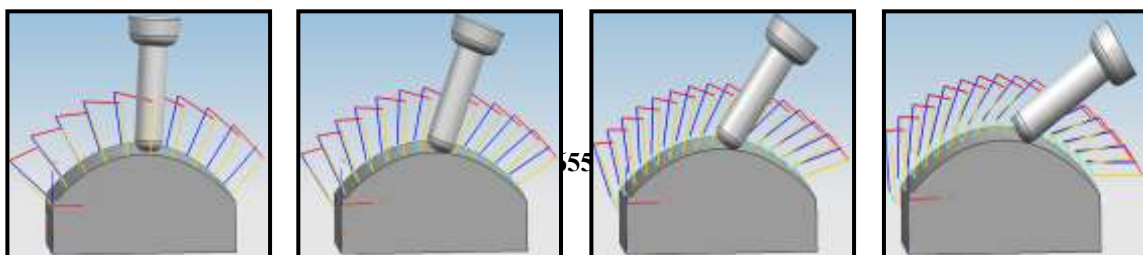
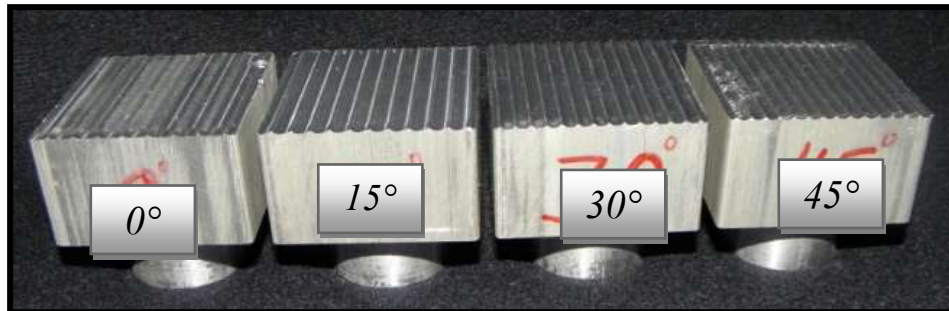
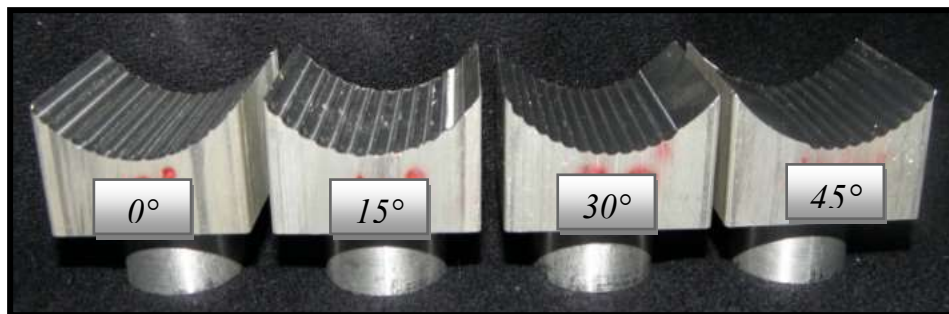


Figure (15 a, b, c and d). The tool path generation of multi-axis CNC milling operation For  $[\lambda = 0^\circ, 15^\circ, 30^\circ \text{ and } 45^\circ]$  respectively for the convex surface.

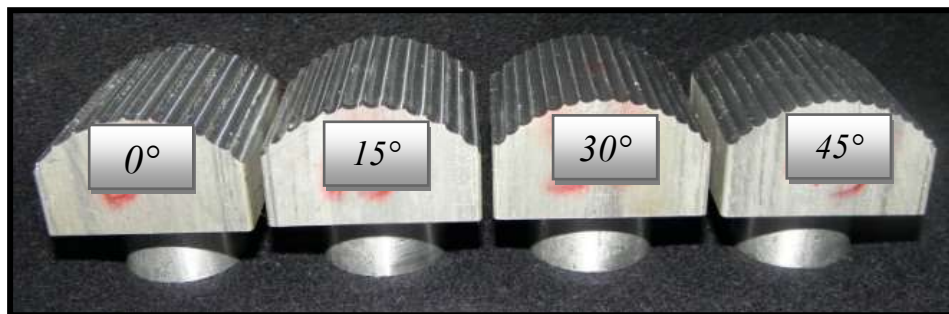




(a) Flat surface.



(b) Concave surface.



(c) Convex surface.

Figure (16 a ,b and c): Explain the specimens that have been implemented in CAD/CAM laboratory at Nanjing University of Aeronautics and Astronautics in China for twelve specimens and the test was divided into three division related to the shape of the specimen profiles, as follow:

- Shape of the specimens profile =3 ( flat, concave, convex)
- Lead angle = $0^{\circ}$  for three type of specimens.
- Lead angle = $15^{\circ}$  for three type of specimens.
- Lead angle = $30^{\circ}$  for three type of specimens.
- Lead angle = $45^{\circ}$  for three type of specimens.

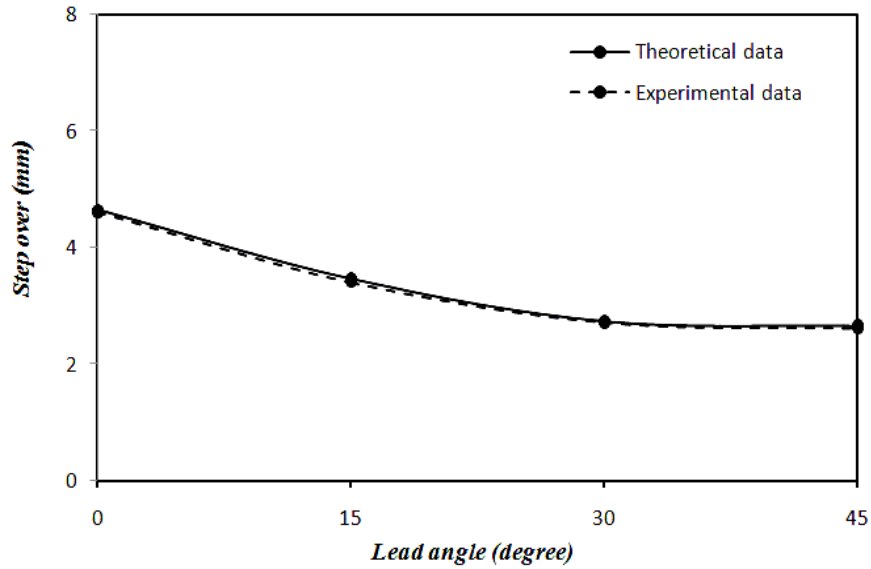


Figure (17). The comparison in results between the theoretical and experimental data relative to the relation between stepover and lead angle.

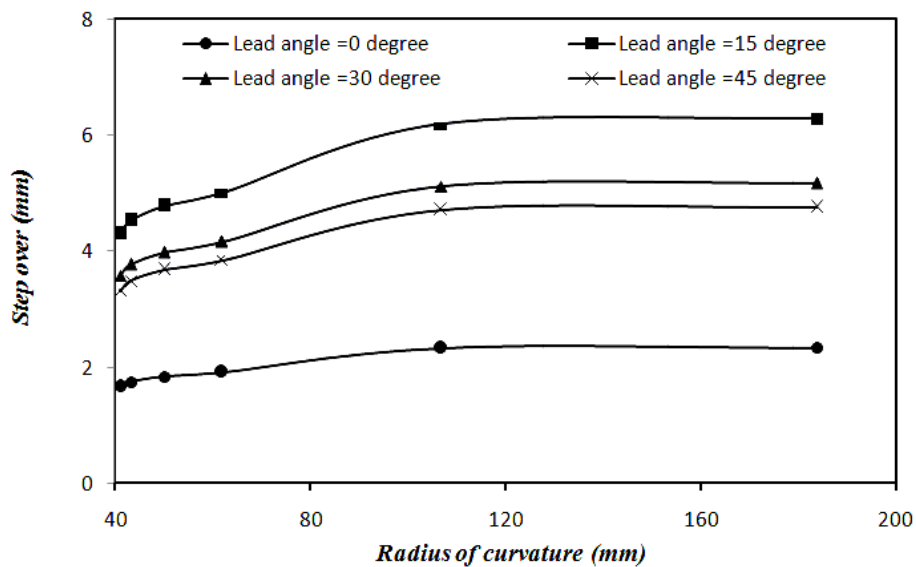


Figure (18). The relation that have been concluded between the step over and radius of curvature of the workpiece relative to lead angle ( $\lambda$ ).

